Boundary conditions and event scaling of granular stick-slip events

Cite as: AIP Conference Proceedings **1145**, 567 (2009); https://doi.org/10.1063/1.3179988
Published Online: 01 July 2009

Karen E. Daniels and Nicholas W. Hayman

Boundary conditions and event scaling of granular stick-slip events

Karen E. Daniels* and Nicholas W. Hayman†

*Department of Physics, North Carolina State University, Raleigh, NC 27695, USA.
†Institute for Geophysics, University of Texas, Austin, TX 78758, USA.

Abstract. We describe experiments on stick-slip failure of a granular material within a linear shear cell. The experiments are performed in a quasi-two-dimensional photoelastic granular material which is sheared via a slider block and spring moving at a constant velocity. The apparatus can provide either constant-volume or constant dP/dV boundary conditions on the aggregate, and we observe boundary-condition dependence in various size-characterizations (duration, force drop, maximum velocity, energy released, area) of the events. Through the use of photoelastic particles, we visualize force chains before and after stick-slip events. We observe that patterns of slip and stress release are highly heterogeneous in their spatial extent, and associate this with scatter in the scaling relations.

Keywords: granular materials, scaling relations, friction
PACS: 61.43.Gt, 81.05.Rm, 83.80.Fg, 81.40.Np, 91.32.Jk, 64.60.av, 62.20.M-

INTRODUCTION

A sheared granular material can respond to external driving by steady motion, periodic motion, or intermittent stick-slip events [1, 2, 3, 4]. This dynamic response involves failure of the frictional contacts among the particles, and is a probe of the frictional properties of the aggregate. One important feature of granular materials is the presence of force chains in which roughly co-linear groups of particles carry more of the load imposed on a granular system than the adjacent particles. Due to this heterogeneous nature of the granular material, the stick-slip events are spatiotemporally complex.

We subject a two-dimensional photoelastic granular material to linear shear and examine the spatial and temporal characteristics of the resulting stick-slip events. We find that multiple distinct "sizes" are useful to characterize these events, among them velocity, force drop, area, energy, and duration. We examine both the extent to which these various measures scale with each other, and how the choice of boundary condition controls this scaling. At the close of this paper, we describe some implications which these studies have for natural, seismogenic faults.

EXPERIMENT

The experiments were performed in a linear shear cell which produces granular-on-granular stick-slip events. An imposed slip plane separates the two halves of a region filled with a two-dimensional granular material, as shown in Figure 1. One side of the aggregate is coupled

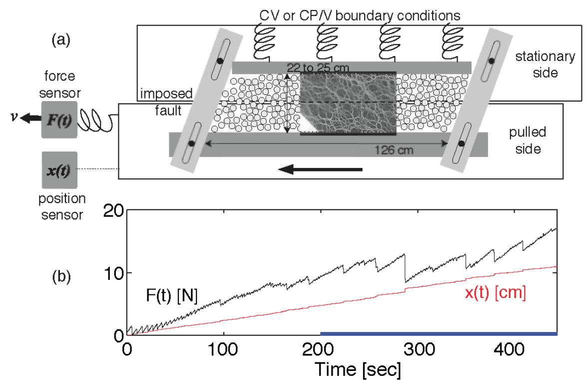

FIGURE 1. (a) Apparatus schematic with force chains as inset in central region. (b) Sample $F(t)$ and $x(t)$ for stick-slip events in CV boundary conditions.

to a stepper motor by a linear spring, and is thus pulled by linear feed screw which moves at a constant velocity of 0.30 mm/s. We record the pulling force $F(t)$ and the plate position $x(t)$. Two boundary conditions for the aggregate are possible: constant volume (referred to as CV) via fixed boundaries and constant dP/dV (CP/V) via confinement with a compressed spring, allowing dilation. More details on the apparatus are available in Daniels and Hayman [5].

We performed 15 experimental runs with CP/V boundary conditions, and 24 runs with CV boundary conditions. Each stick slip event is system-spanning, in that shear must have taken place along the full length of the imposed fault in order to produce a forward slip of the plate. For each slip event, we see a corresponding drop

CP1145, *Powders and Grains 2009, Proceedings of the 6th International Conference on Micromechanics of Granular Media* edited by M. Nakagawa and S. Luding

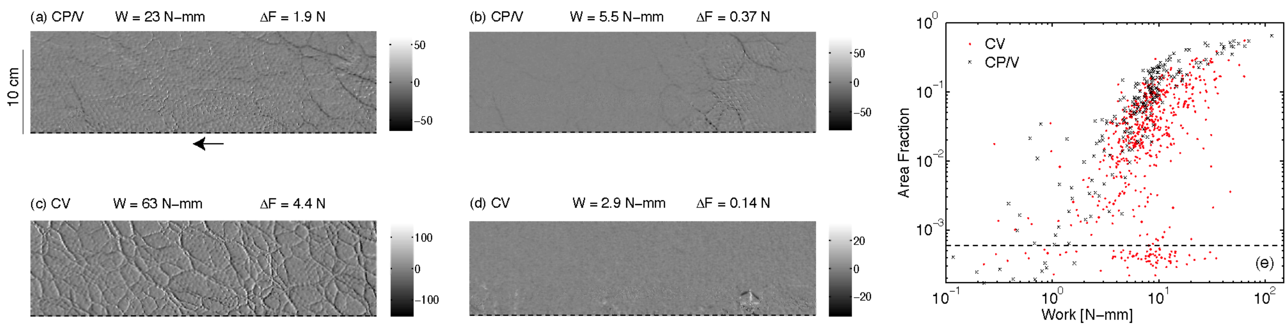

FIGURE 2. (a-d) Sample image-differences of the stationary side of the apparatus for various boundary conditions and event sizes. On each image, the imposed fault plane is indicated by a black dashed line along the bottom edge; the scale bars represent the change in the intensity value of a pixel during the event, out of a possible 8 bits (256 units) of intensity. (e) Event work vs. participating area fraction. Dashed line represents the area fraction for a single particle.

in the pulling force. A side-by-side comparison of sample $F(t)$ and $x(t)$ signals is shown in Figure 1. Note that under both boundary conditions, the granular material strengthened and developed a force-chain network through approximately periodic stick-slip motion during an initial period of ≈ 200 seconds. Once the internal stresses were well-established, the experiments entered a regime of aperiodic behavior, marked by the thick bar along the time axis. This is the regime from which we collected data, resulting in ≈ 1500 stick-slip events for each boundary condition. In the case of CP/V events (not shown), there was much less strengthening during this later phase, due to the ability of the system to dilate and thus relieve internal stresses. Movies of the dynamics are available online [5].

RESULTS

We detect individual events using the timeseries dF/dt and dx/dt, calculated by first smoothing the original series using a window of 0.6 seconds and then utilizing Fourier-space derivatives to avoid triggering events on the basis of noise. We locally fit a parabola to all events above a threshold, and from this fit determine the start time t_1, the end time t_2 and the duration T. We measure the (positive) drop in the pulling force $\Delta F = F(t_1) - F(t_2)$ (measured in Newtons) and a work term (measured in N-mm): $W = \sum_{i=t_1}^{t_2} F_i\,(x_{i+1} - x_i)$. These three values ($T$, ΔF, W) were extracted for each event, discarding small events of the wrong sign as well as events from the initial 200 seconds of force buildup. Note that because every stick slip event displaces the entire shear zone boundary, the rupture length L is constant for all events.

To examine the spatial extent of the failure during each event, we subtract an image of the stationary side taken at t_1 from the image at t_2. Example images are shown in Figure 2(a-d). Each event is composed of particle displacements and/or changes in the strengths of force chains. The difference images appear white where a force chain strengthened, black where a force chain weakened, and gray where no change occurred. A chain that is lined with a white strip on the left side and dark on the right slipped sideways as a unit, while particles that slipped sideways appear as faint rings. We observe a great deal of heterogeneity in the spatial extent and location of both types of failure, but in general the larger W, the larger the proportion of the granular material participated in the event. For the largest events, particularly in the CV boundary conditions, system-spanning rearrangements are commonly observed, often with some sliding along the shear-zone boundaries (as in Figure 2(c)).

We quantify this effect by considering the fractional area A of these images that exhibited an above-threshold change in pixel brightness. This semi-quantitative estimate is plotted in Figure 2(e), and we observe a strong correlation between the two quantities, particularly for $W \gtrsim 5$ N-mm. The horizontal dotted line marks the value of A corresponding to a single particle and we observe a breakdown in the scaling for values of A larger than a few particle areas. This value is consistent with a patch the approximate width of the shear band. We do not observe a significant difference in behavior for events taking place in the two different boundary conditions.

In Figure 3, we compare sizes ΔF and W for events from the two different boundary conditions. For values of $\Delta F \gtrsim 0.2$ N (the median value of ΔF), we observe an approximately linear relationship between the two sizes. This is to be expected, since both ΔF (through the spring coupling) and W are likely proportional to the slip during the events; more details about this relationship are discussed in Daniels and Hayman [5]. However, the proportionality is only valid on average and the constant of proportionality λ weakly depends on the choice of boundary condition. This coefficient λ has units of length and ranges from 3 to 100 mm for the dashed lines shown in

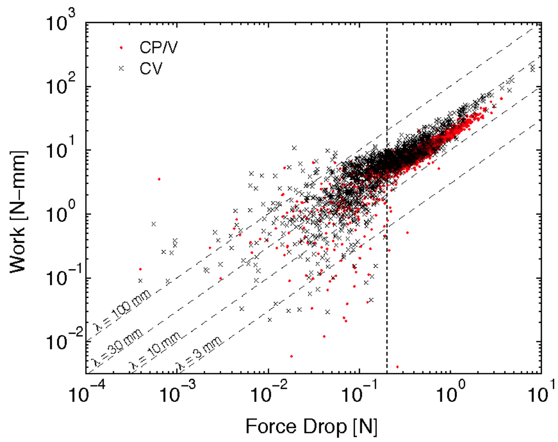

FIGURE 3. Scaling relationship between force drop ΔF and work W, with dashed lines indicating $W = \lambda \Delta F$ for four values of λ. Vertical dotted line denotes breakdown in scaling regime, near the median value of ΔF.

Figure 3, with a larger value observed for the CV boundary conditions. One possible interpretation is that different amounts or numbers of particle-scale slips occur in different events, which might be detectable in a more detailed analysis along the lines of Figure 2. The CPV boundary conditions are observed to have fewer strong force chains, providing some evidence that fewer slips may be present.

Finally, we examine scaling in the rates at which the events occur. Each event starts from a jammed state, begins to fail after the pulling force rises past a critical value, slips for a duration T, and then returns to the jammed state and the cycle begins again. We observe the velocity (dx/dt) of the pulled plate as a function of time to examine scaling in the maximum velocity reached during slip. Because the signals are quite noisy, we compare pulse shapes on average rather than individually. We sort the events by duration T, bin them into groups of 25 events of similar duration, and within each bin we rescale and average the signals.

Figure 4(a-b) shows average pulse shapes (for each boundary condition, and only for $\Delta F > 0.2$ N), which have been scaled by both duration and maximum velocity in order to collapse the data. We observe similarity in the shapes, independent of boundary condition, with clear evidence of a maximum, sustained velocity during the middle of each event. In Figure 4(c), we observe that while the CP/V events show non-monotonic dependence of maximum velocity on duration, for CV boundary conditions the maximum velocity scales with the duration of the event. Such scaling is characteristic of crackling noise, which typically arises in situations where a disordered system with many degrees of freedom is subjected to slow forcing, producing discrete failure events with a wide variety of sizes [6].

DISCUSSION

We have presented a sampler of the kinds of scaling relations present and absent in various quantities describing the size of stick-slip events. Interestingly, in Daniels and Hayman [5], we previously observed that ΔF and W have power-law distributions for CV boundary conditions, but exponential distributions for CPV boundary conditions. While the CV runs strengthen significantly over time (and the CP/V do not), the distributions of W and ΔF are stationary. We observe that work W, force drop ΔF, and participating area A all scale with each other for events above a minimum size. A second type of observed scaling involves the slip rate and the duration, which for CV (but not CP/V) boundary conditions display behavior reminiscent of cracking noise. The presence of such scaling relations provides a promising direction for future research into its origins.

Nonetheless, both the scaling regimes and the quality of scaling are imperfect. In spite of the fact that all events rupture the full length of the imposed fault, for any given event energy there is a range of observed spatial extents, as shown in Figure 2. Similarly, the value of λ relating ΔF to W (Figure 3) ranges from 10 to 50 mm, even within the upper scaling regime. This breakdown/scatter in the scaling relations suggest that there are multiple ways in which to create a "large" event: force chain releases and particle-slips have independent (but likely correlated) contributions to the size.

For the smaller events ($\Delta F \lesssim 0.2$ N), the work W no longer scales with ΔF or A, and instead shows little correlation. These small event sizes correspond to generally local force-chain changes rather than the system-spanning changes observed for larger size events and probability reveals information about particle-particle interactions rather than the overall stress state of the system. It is only the larger events which are affected by both particle and force-chain rearrangements. Since these larger events involve force chains which span the system, they have an enhanced sensitivity to the boundary conditions.

These results connect to the geophysics of natural faults in several important ways. First, the events exhibit statistical properties (power law size distributions) similar to those observed in natural earthquake populations, such as the Gutenberg-Richter (frequency-moment) relation, which has also been observed in granular experiments with constant *pressure* (CP) boundary conditions [3, 4]. This observation is not unexpected: the geometry of the experiment is analogous to a natural, gouge-filled strike-slip fault. However, we observed that these

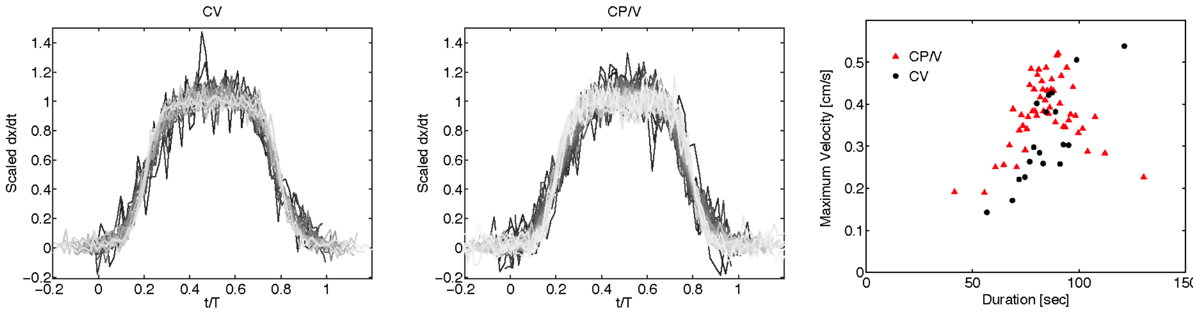

FIGURE 4. (a,b) Velocity pulses for events of different duration, scaled by v_{max} and T. Each line is the average of 25 events with (dark $\rightarrow$ light) shading corresponding to (short $\rightarrow$ long) duration. (c) Duration and magnitude used for the collapse of velocity pulse curves in (a,b).

power-law distributions were not universal: the pulling force drop ΔF and event energy W only have power law tails for CV boundary conditions. In addition, we observed a breakdown in the scaling relation for ΔF and W which may be related to the observation that smaller earthquakes typically have a wider range of stress drops than the largest ones [7] as was similarly observed in Figure 3. Further geological and seismological and implications are discussed in Daniels and Hayman [5].

ACKNOWLEDGMENTS

We thank Peter Malin, Robert Behringer, and Peidong Yu for discussions surrounding the development of the experiments, and Greg Gibson for assistance in constructing the apparatus. K.D. received support from NC State University and NSF-DMR 0644743 and N.H. received support from NSF-OCE 0222154 (to Jeffrey Karson) and the University of Texas, Institute for Geophysics of the Jackson School for Geosciences.

REFERENCES

1. F. Heslot, T. Baumberger, B. Perrin, B. Caroli, and C. Caroli, *Physical Review E* **49**, 4973–4988 (1994), URL `http://link.aps.org/abstract/PRE/v49/p4973`.
2. S. Nasuno, A. Kudrolli, and J. P. Gollub, *Physical Review Letters* **79**, 949–952 (1997), URL `http://link.aps.org/abstract/PRL/v79/p949`.
3. P. Yu, and R. P. Behringer, *Chaos* **15**, 041102 (2005), URL `http://link.aip.org/link/?CHA/15/041102`.
4. M. Bretz, R. Zaretzki, S. B. Field, N. Mitarai, and F. Nori, *Europhysics Letters* **74**, 1116–1122 (2006), URL `http://stacks.iop.org/0295-5075/74/1116`.
5. K. E. Daniels, and N. W. Hayman, *Journal of Geophysical Research* **113**, B11411 (2008), movies available at http://www.agu.org/journals/jb/jb0811/2008JB005781/displays.shtml.
6. J. P. Sethna, K. A. Dahmen, and C. R. Myers, *Nature* **410**, 242–250 (2001).
7. R. E. Abercrombie, *Journal of Geophysical Research* **100**, 24015–20036 (1995).